Reply to Anonymous Referee #1

We thank the reviewer for the careful reading of the manuscript and helpful comments. We have revised the manuscript following the suggestion, as described below.

Wang et al. investigate the monthly and spatial variability of ozone (O_3) formation in the Guanzhong Basin and discuss implications for mitigating O_3 and secondary aerosol pollution. The study combines in situ observations with WRF-Chem simulations and includes analyses of EKMA regimes and source contributions. Overall, the approach is sound and the analyses are carefully conducted. I recommend minor revision before publication.

1. My first comment is about the application of EKMA isopleth profiles to MDA8 O_3. EKMA analyses are most commonly applied to O_3 production rates, with the goal of quantifying the sensitivity of local photochemical O_3 production to local NO_x and VOC emissions. In this study, EKMA is applied directly to MDA8 O_3, which includes not only local chemical production but also the effects of transport and advection. It would be helpful for the authors to discuss the extent to which transport and advection may influence the EKMA results, and to clarify why this approach is appropriate for MDA8 O_3 in the present context.

Response: We thank the reviewer for this insightful comment. We agree that EKMA is originally devised in the context of O_3 production and that MDA8 O_3 might include contributions from transport. We have added explanations in Section 2.3 and discussions in Section 3.3 of the revised manuscript as follows,

L98-104: "*The high-resolution, online-coupled WRF-Chem framework simulates all key processes affecting O_3 formation (local photochemistry, regional transport, vertical mixing) consistently. By varying emissions under fixed meteorology and boundary conditions, the model isolates the net impact of emission changes on MDA8 O_3 concentrations. While the classical EKMA method based on O_3 production rates reflects a more localized chemical mechanism, our approach provides an integrated,*

policy-relevant sensitivity diagnosis that accounts for both formation and transport at the urban-regional scale, offering directly actionable insight for control strategies (Ye et al., 2025)."

L107-113: "*In the present study, MDA8 O_3 concentrations are used as the response metric in chemical regime identification and source apportionment for several key reasons. First, MDA8 O_3 represents the period of highest daily O_3 exposure, offering a robust indicator of actual O_3 pollution levels. Second, it is the official metric for ambient O_3 standards under China's national air quality regulations. Assessing how MDA8 O_3 responds to emission perturbations therefore provides direct, policy-relevant insights for designing effective air quality management and control strategies.*"

L258-276: "*It is important to recognize that MDA8 O_3 variations in the EKMA diagrams integrate contributions from both local photochemical production and atmospheric transport and advection. Multiple recent modeling studies demonstrate that transport processes can contribute substantially to the regional O_3 burden. For example, concentration and mass budget analyses show that horizontal advection from upwind regions and entrainment from the residual layer can supply a significant portion of O_3 mass to a receptor region, especially during morning hours or under synoptic transport conditions, even if local photochemistry subsequently drives the daytime increase in surface O_3 (Qu et al., 2023). In the study, the design of EKMA simulations isolates the chemical sensitivity to precursor emissions by holding the meteorological fields and chemical boundary conditions fixed across all scenarios. Because circulation and transport are invariant in this framework, changes in MDA8 O_3 arising from systematic reductions in NO_X and VOCs emissions mainly reflect the in-situ chemical response of O_3 formation rather than changes in transport dynamics.*

It is worth noting that transport and advection represent a background forcing for region O_3 concentrations. Studies of tropospheric O_3 and its precursors emphasize that long-range transport of O_3 and its precursors can influence surface O_3 trends and variability, and that such transport sets the baseline on which local chemistry operates

(Han et al., 2019; Garatachea et al., 2024; Chen et al., 2025). These transport influences can bias the placement of EKMA isolines in cases where background precursor concentrations (e.g., high transported NO_X or VOCs) differ substantially from typical values, potentially shifting the diagnosed sensitivity toward VOCs-limited or NO_X-limited regimes under certain conditions (Elshorbany et al., 2024). In this study, to mitigate the influence of transport and advection on EKMA results, we select representative O_3 pollution days that exclude anomalous episodes with unusually high backgrounds of transported O_3 and its precursor, such as strong synoptic advection or intrusion events. Hence, the EKMA diagnostics primarily capture the local chemical response to precursor perturbations under typical regional circulation patterns."

Reference:

Chen, C., Chen, W., Guo, L., Wu, Y., Duan, X., Wang, X., and Shao, M.: A comprehensive review of tropospheric background ozone: definitions, estimation methods, and meta-analysis of its spatiotemporal distribution in China, Atmos. Chem. Phys., 25, 15145–15169, doi:10.5194/acp-25-15145-2025, 2025.

Elshorbany, Y., Ziemke, J. R., Strode, S., Petetin, H., Miyazaki, K., De Smedt, I., Pickering, K., Seguel, R. J., Worden, H., Emmerichs, T., Taraborrelli, D., Cazorla, M., Fadnavis, S., Buchholz, R. R., Gaubert, B., Rojas, N. Y., Nogueira, T., Salameh, T., and Huang, M.: Tropospheric ozone precursors: global and regional distributions, trends, and variability, Atmos. Chem. Phys., 24, 12225–12257, doi:10.5194/acp-24-12225-2024, 2024.

Garatachea, R., Pay, M. T., Achebak, H., Jorba, O., Bowdalo, D., Guevara, M., Petetin, H., Ballester, J., and Pérez García-Pando, C.: National and transboundary contributions to surface ozone concentration across European countries, Commun. Earth Environ., 5, 588, doi:10.1038/s43247-024-01716-w, 2024.

Han, H., Liu, J., Yuan, H., Wang, T., Zhuang, B., and Zhang, X.: Foreign influences on tropospheric ozone over East Asia through global atmospheric transport, Atmos. Chem. Phys., 19, 12495–12514, doi:10.5194/acp-19-12495-2019, 2019.

Qu, K., Wang, X., Cai, X., Yan, Y., Jin, X., Vrekoussis, M., Kanakidou, M., Brasseur, G. P., Shen, J., Xiao, T., Zeng, L., & Zhang, Y. Rethinking the role of transport and photochemistry in regional ozone pollution: Insights from ozone concentration and mass budgets. Atmos. Chem. Phys., 7653–7671. https://doi.org/10.5194/acp-23-7653-2023, 2023.

2. My second comment relates to the source attribution methodology. It is unclear whether the O_3 attributed to individual source sectors is calculated by completely removing the corresponding emission source and comparing against the base case, or by incrementally reducing emissions. Additional discussion of how chemical nonlinearity in O_3 formation may affect the source attribution would strengthen this part of the analysis.

Response: We appreciate the reviewer's query regarding the source attribution details. In the BFM application, we have completely removed one sector at a time (industry, power, traffic, residential, biogenic) in separate sensitivity simulations, and compared the resulting MDA8 O_3 and SA concentrations against the base case. We have clarified in Section 2.3 as follows,

L105-107: "*The BFM calculates the contribution of a specific source sector by completely removing (setting to zero) all emissions from that sector in the base simulation and comparing the resulting MDA8 O_3/SA concentration with the base case (Dunker et al., 1996).*"

We fully agree with the reviewer that chemical nonlinearity is a critical consideration. To address this, we have added a new paragraph in Section 3.4 discussing this limitation.

L321-336: "*The source contributions presented in this study are quantified using the BFM, wherein emissions from a specific sector are entirely removed to evaluate its potential impact on O_3 concentrations. While this approach is effective for assessing the control potential of individual sources and is widely used in policy-relevant scenario analysis, it is important to consider the inherent nonlinearity of tropospheric O_3 chemistry. The response of O_3 concentrations to a given emission change depends strongly on the background chemical regime (NO_X- vs. VOCs-limited, as shown in Section 3.3). For example, in a VOCs-limited regime, reducing NO_X emissions alone may inadvertently increase O_3 concentrations, whereas the same reduction in a NO_X-limited regime would lower O_3 concentrations. Consequently, the attribution*

derived from complete removal of a source may not scale linearly with incremental emission controls. As discussed in Li et al. (2023), when emission perturbations are large, the assumption of a linear response between emission change and O_3 change becomes invalid due to the nonlinear interactions in O_3 production chemistry, meaning that attribution results from BFM may differ from those obtained by alternative methods such as source tagging that explicitly follow chemical pathways. Importantly, BFM and tagging methods answer different scientific questions that the BFM estimates the sensitivity of O_3 to sector-specific emission changes, whereas tagging method attributes the total mass of O_3 to source precursors independent of changes in emissions (Li et al., 2023; Shu et al., 2023). In this study, the BFM results are interpreted in conjunction with the OFR analysis (Section 3.3), which delineates the nonlinear photochemical sensitivity to gradual precursor changes. Together, they provide a robust basis for identifying priority source sectors and designing effective, regime-specific control strategies for the GZB."

Reference:

Li, P., Yang, Y., Wang, H., Su, L., Li, S., et al.: Source attribution of near-surface ozone trends in the United States during 1995–2019, Atmos. Chem. Phys., 23, 5403–5417, doi:10.5194/acp-23-5403-2023, 2023.

Shu, Q., Napelenok, S. L., Hutzell, W. T., Baker, K. R., Henderson, B. H., Murphy, B. N., and Hogrefe, C.: Comparison of ozone formation attribution techniques in the northeastern United States, Geosci. Model Dev., 16, 2303–2322, doi:10.5194/gmd-16-2303-2023, 2023.

3. Finally, the structure of the Results section, particularly Section 3.3, could be improved for clarity. While the descriptions of individual figures are thorough, the section is quite dense. In particular, a clearer separation of the roles of local meteorology (largely uncontrollable) versus emissions (policy-relevant factors) across different cities and months would help readers better follow the key messages.

Response: We thank the reviewer for the constructive suggestion to improve the clarity

of the Results section. We have thoroughly revised Section 3.3 by dividing it into subsections to better separate the roles of meteorological drivers and emission-related factors. The revised sections are as follows,

L173-276: "3.3 *Spatiotemporal Patterns of O_3 Sensitivity from EKMA Analysis*

O_3 formation in the planetary boundary layer (PBL) is a complex and nonlinear process driven by sunlight acting on NO_X and VOCs. Figures 3 and 4 present EKMA diagrams for four high-O_3 pollution episodes from May to August 2022 in urban areas of the GZB and its five cities, respectively. These diagrams depict O_3 isopleths for OFR identification, derived from sensitivity simulations with systematically reduced NO_X and AVOCs emissions. The ridge line (red lines) delineates the boundary between these regimes: scenarios above it lie in the VOCs-limited regime (O_3 falls more with AVOCs cut), those below in the NO_X-limited regimes, and scenarios near the line are transitional regimes (mixed sensitivity). The upper-right corner (100% AVOCs, 100% NO_X emissions) represents the current emission scenario, whose location relative to the ridge line determines the prevailing sensitivity regime.

3.3.1 Spatiotemporal Shifts in OFR

EKMA curves reveal a pronounced sub-seasonal progression of OFR across the GZB. In May and June, the basin as a whole is predominantly VOCs-limited, indicating AVOCs reductions would substantially lower O_3 concentrations, whereas moderate NO_X cuts could exacerbate O_3 pollution (Figs. 3a, 3b). By July, OFR in urban areas shifts toward a transitional regime (Fig. 3c). In August, the GZB enters a NO_X-limited regime (Fig. 3d), where a 40% NO_X reduction yields an 11.1% decrease in MDA8 O_3, compared to only 3% for an equal AVOCs cut. City-scale analyses show marked spatial heterogeneity (Fig. 4). In early summer, XA, XY, WN, and TC exhibit VOCs-limited regimes. BJ generally falls within NO_X-limited or transitional regimes. WN is the most NO_X-saturated (VOCs-limited) city. By August, OFRs in all cities except WN (transitional) become NO_X-limited.

To assess the robustness of the simulated sub-seasonal OFR progression against

interannual variability in meteorology and emissions, we further examine the formaldehyde-to-NO_2 ratio (FNR) from satellite retrievals for the GZB region over three consecutive warm seasons (2021-2023). FNR is a widely used indicator for inferring near-surface O_3 sensitivity, with thresholds typically defined as: FNR < 1 for VOCs-limited, 1–2 for transitional, and >2 for NO_X-limited regimes (Jin et al., 2015; Hata et al., 2025; Rahman et al., 2025). The monthly FNRs reveal a consistent sub-seasonal evolution pattern across the three years. The spatial distributions transition from being dominated by blue grids (low FNR, VOCs-limited) in early summer to more green (transitional) and eventually yellow/red grids (NO_X-sensitive) by late summer, particularly evident in 2021 and 2022 (Fig. S6). At the basin scale, the mean FNR increases consistently from May to August, from 0.90 to 1.61 in 2021 and from 0.91 to 1.77 in 2022, reflecting a systematic seasonal shift toward more NO_X-limited O_3 formation (Table S3). Despite data gaps in May and August 2023, FNR values of 1.20 in June and 1.43 in July indicate a similar transition from transitional to more NO_X-sensitive conditions. Note that although column-based FNR is a useful indicator of surface O_3 sensitivity, satellite retrievals are subject to substantial uncertainties arising from measurement errors, cloud contamination, surface reflectivity, profile assumptions, and aerosol effects (Jin et al., 2017; Souri et al., 2023).

This independent, multi-year satellite evidence provides strong support for the central finding of our model-based analyses, namely a recurring sub-seasonal transition in O_3 formation regimes over the GZB, evolving from VOCs-limited conditions in early summer to transitional and ultimately NO_X-limited regimes by late summer. The consistency of this progression across years with contrasting meteorological conditions, including the extreme heat in 2022, indicates that the diagnosed regime shift is a robust characteristic of the regional photochemical environment. This behavior is therefore more plausibly driven by sub-seasonal factors, such as enhanced solar radiation, higher temperatures, and increased biogenic emissions, rather than by year-specific meteorological or emission anomalies.

3.3.2 Drivers of Temporal Shifts: Meteorology and Associated Chemistry

The temporal OFR transition from VOCs-limited to NO_X-limited is primarily

driven by evolving meteorology and chemistry from May to August. The AVOCs/NO_X emission ratios are relatively stable (0.27-0.34; Table S4) during the warm season. This variation cannot explain the stronger NO_X sensitivity detected in July–August, indicating that anthropogenic precursor ratios alone do not fully account for the seasonal OFR shifts. The most important change from May to August is the intensification of solar radiation and the resultant increase in air temperature. Firstly, BVOCs emissions are dependent on solar radiation and air temperature, so increased solar radiation and air temperature in mid-late summer boost BVOCs emissions, providing more background VOCs and pushing the O_3 formation toward NOx-sensitive. Secondly, enhancement of solar radiation and higher temperature accelerate photochemical reactions. In addition, higher temperatures favor a deeper PBL, which enhances vertical mixing and can entrain O_3-rich air from aloft while diluting near-surface precursor concentrations and thus altering local precursor ratios. Near-surface O_3 concentrations tend to increase as the PBL height (PBLH) increases, peaking at the PBLH of approximately 900-1800 m (Wang et al., 2023). In urban areas of the GZB, the mean PBLH during 11:00-18:00 BJT rises from 1382 m in May to 1720 m in June, then falls to 1412 m in July and 1406 m in August, consistent with the maximum MDA8 O_3 level in June. Simulations indicate that HO_X radical concentrations increase while near-surface NO_X levels decrease from May to August in urban areas of the GZB (Fig. 5 and Table S5). These changes are closely linked to enhanced BVOCs emissions, intensified atmospheric photochemistry and PBL development, which alter relative balance of the O_3 precursor levels. Consequently, HO_X-loss becomes increasingly dominated by self-reaction of peroxyl radicals rather than $HO\cdot + NO_2$ termination, further shifting O_3 production to be more NO_X-sensitive.

The similar transition trend has been found in previous studies. Wu and Xie (2017) have discussed occurrence of a switch from a NO_X-saturated to NO_X-sensitive O_3 formation regime in most suburban and rural areas in China when summer arrives. Ou et al. (2016) have proposed that O_3 formation shifts toward VOCs-limited conditions in the PRD from summer to autumn. Sun et al. (2018) have used high-resolution observations in eastern China to show that the photochemical regime during spring

and summer tends toward NO_X-limited or mixed sensitivity, while in autumn and winter it shifts toward VOCs-limited conditions. Our study extends this understanding by resolving OFR transitions at sub-seasonal (monthly) and city-specific levels, offering feasible insights for dynamic emission control.

3.3.3 Drivers of Spatial Heterogeneity: Emissions and Transport

Spatial differences in OFR are closely tied to local emission profiles and regional transport. A key factor is the local VOCs (AVOCs + BVOCs) / NOx emission ratio (Fig. 6). In early summer, XA, XY, WN, and TC had low ratios (2–7), leading to VOCs-limited regimes due to high NO_X emissions. In contrast, BJ's higher ratio (11–29) corresponds to NO_X-limited or transitional regimes. Notably, the strong VOCs sensitivity in WN is consistent with its relatively low VOCs/NO_X ratio, reflecting elevated NO_X emissions from intensive power plant in the region. This pattern echoes observations in other heavily polluted Chinese cities, which often show strong VOCs sensitivity. These contrasts underscore that effective control strategies must account for both local emissions and inter-regional transport. This inflow elevates local NO_X (with relatively longer atmospheric lifetime than that of reactive VOCs) concentrations relative to VOCs, emphasizing the necessity of targeted AVOCs reductions before aggressive NO_X cuts can effectively mitigate O_3 pollution in this city.

These intra-region contrasts underscore that control strategies must be tailored to local chemistry. Similar patterns occur elsewhere: Ren et al. (2022) have found heavily polluted Chinese cities (e.g. Wuhan, Xi'an) are strongly VOCs-limited, whereas suburb and rural areas are NO_X-limited. Likewise, Yu et al. (2025) have diagnosed Zhengzhou's O_3 regime as primarily VOCs-limited, with an optimal ratio of VOCs to NO_X emission reductions of approximately 2.9:1, consistent with the strong VOC sensitivity observed in industrialized cities. Likewise, Yu et al. (2025) have diagnosed Zhengzhou's O_3 formation regime as primarily VOCs-limited, with an optimal VOCs-to-NO_X reduction ratio of approximately 2.9:1, consistent with the strong VOC sensitivity observed in industrialized cities.

Overall, these spatial and sub-seasonal OFR shifts highlight the necessity of dynamic, month-specific O_3 control strategies in the GZB. The pronounced VOCs-

limited conditions in early summer call for prioritizing AVOCs control, especially in cities with sever O_3 pollution like WN and XA, while the transition to NO_X-limited conditions by late summer favors NO_X-focused measures. Such temporally and spatially optimized approaches could enhance the efficiency of regional O_3 mitigation and help avoid unintended increases during seasonal transitions.

It is important to recognize that MDA8 O_3 variations in the EKMA diagrams integrate contributions from both local photochemical production and atmospheric transport and advection. Multiple recent modeling studies demonstrate that transport processes can contribute substantially to the regional ozone burden. For example, concentration and mass budget analyses show that horizontal advection from upwind regions and entrainment from the residual layer can supply a significant portion of ozone mass to a receptor region, especially during morning hours or under synoptic transport conditions, even if local photochemistry subsequently drives the daytime increase in surface ozone (Qu et al., 2023). However, the design of our EKMA simulations isolates the chemical sensitivity to precursor emissions by holding the meteorological fields and boundary conditions fixed across all scenarios. Because circulation and transport are invariant in this framework, changes in MDA8 O_3 arising from systematic reductions in NO_X and VOCs emissions reflect the in-situ chemical response of O_3 formation rather than changes in transport dynamics.

It is well-recognized that transport and advection represent a background forcing for region O_3 concentration. Studies of tropospheric O_3. precursors emphasize that long-range transport of O_3 and its precursors can influence surface O_3. trends and variability, and that such transport sets the baseline on which local chemistry operates. These transport influences can bias the placement of EKMA isolines in cases where background precursor concentrations (e.g., high transported NO_X or VOCs) differ substantially from typical values, potentially shifting the diagnosed sensitivity toward VOCs-limited or NO_X-limited regimes under certain conditions (Elshorbany et al., 2024). In this study, to mitigate the influence of transport and advection on EKMA results, we select representative O_3 polluted days that exclude anomalous episodes with unusually high backgrounds of transported O_3 and its precursor, such as strong

synoptic advection or intrusion events. Hence, the EKMA diagnostics predominantly capture the local chemical response to precursor perturbations under typical regional circulation patterns."

Reply to Anonymous Referee #2

We thank the reviewer very much for the careful reading of our manuscript and helpful comments. We have revised the manuscript following the suggestions, as described below.

This manuscript investigates the sub-seasonal and spatial variability of ozone and secondary aerosol formation regimes in the Guanzhong Basin from May to August 2022 based on WRF-Chem simulations and EKMA curves. The key finding is a sub-seasonal progression in O_3 sensitivity (VOC-limited --> transitional --> NO_x-limited) and policy implications for month- and city-specific controls. While the novelty of the approach is somewhat limited, the analysis of sub-seasonal regime shifts is timely and carries important policy relevance for regional air quality management. The manuscript is generally well written, and the methods are sound. I recommend publication after the following major and minor issues are addressed.

1. The policy implications of this study are largely based on simulations for a single year (2022). However, 2022 was one of the warmest years in China since 1961, characterized by intense heatwaves and drought, and emissions in 2022 may also differ from other years (e.g., 2019 or 2024) due to COVID-related impacts. Given the strong sensitivity of ozone formation to both meteorology and emissions, it is unclear whether the diagnosed regime shifts and associated policy implications are representative of other years. The authors are encouraged to discuss the robustness of their conclusions to interannual variability in meteorology and emissions. Where feasible, additional support using observations combined with indicator-based methods or box-model analyses could help verify the ozone formation regimes in 2022 and assess their consistency with other recent years.

Response: We sincerely thank the reviewer for raising this critical point regarding the potential influence of interannual variability in meteorology and emissions on our conclusions, which are primarily based on simulations for 2022. We agree that ensuring the robustness of the diagnosed ozone formation regime (OFR) shifts is essential for

deriving reliable policy implications.

To address this concern, utilizing the multi-year satellite data, we have calculated the monthly mean formaldehyde-to-NO_2 ratio (FNR), a widely used proxy for near-surface O_3 sensitivity, over the GZB for the warm seasons of 2021, 2022, and 2023. The FNR is derived from tropospheric column densities of HCHO and NO_2 retrieved by the OMI sensor. We have added data description in Section 2.2 and results and discussions in Section 3.3.1 as follows,

L87-91: "*To evaluate the robustness of the simulated OFR, we have employed satellite-derived column densities of formaldehyde (HCHO) and NO_2. Daily Level-3 gridded HCHO data are obtained from the OMI/Aura HCHO Total Column Daily L3 Global 0.1°×0.1° product (OMHCHOd v003; NASA GES DISC). Daily Level-3 gridded NO_2 data are sourced from the OMI/Aura NO_2 Cloud-Screened Total and Tropospheric Column L3 Global 0.25°×0.25° product (OMNO2d v003; NASA GES DISC). A grid cell is excluded from the monthly average calculation if valid data are available for fewer than 8 days in that month.*"

L191-210: "*To assess the robustness of the simulated sub-seasonal OFR progression against interannual variability in meteorology and emissions, we examined the formaldehyde-to-NO_2 ratio (FNR) from satellite retrievals for the GZB region over three consecutive warm seasons (2021-2023). FNR is a widely used indicator for inferring near-surface O_3 sensitivity, with thresholds typically defined as: FNR < 1 for VOCs-limited, 1–2 for transitional, and >2 for NO_X-limited regimes (Jin et al., 2015; Hata et al., 2025; Rahman et al., 2025). The monthly FNRs reveal a consistent sub-seasonal evolution pattern across the three years. The spatial distributions transition from being dominated by blue grids (low FNR, VOCs-limited) in early summer to green (transitional) and eventually yellow/red grids (NO_X-sensitive) by late summer, particularly evident in 2021 and 2022 (Fig. S6). At the basin scale, the mean FNR increased consistently from May to August, from 0.90 to 1.61 in 2021 and from 0.91 to 1.77 in 2022, reflecting a systematic seasonal shift toward more NO_X-limited O_3*

formation (Table S3). Despite data gaps in May and August 2023, FNR values of 1.20 in June and 1.43 in July indicate a similar transition from transitional to more NO_X-sensitive conditions. Note that although column-based FNR is a useful indicator of surface O_3 sensitivity, satellite retrievals are subject to substantial uncertainties arising from measurement errors, cloud contamination, surface reflectivity, profile assumptions, and aerosol effects (Jin et al., 2017; Souri et al., 2023).

This independent, multi-year satellite evidence provides strong support for the central finding of our model-based analysis, namely a recurring sub-seasonal transition in O_3 formation regimes over the GZB, evolving from VOCs-limited conditions in early summer to transitional and ultimately NO_X-limited regimes by late summer. The consistency of this progression across years with contrasting meteorological conditions, including the extreme heat in 2022, indicates that the diagnosed regime shift is a robust characteristic of the regional photochemical environment. This behavior is therefore more plausibly attributable to recurrent seasonal drivers, such as increasing solar radiation, temperature, and biogenic emissions, rather than to anomalies associated with any single year."

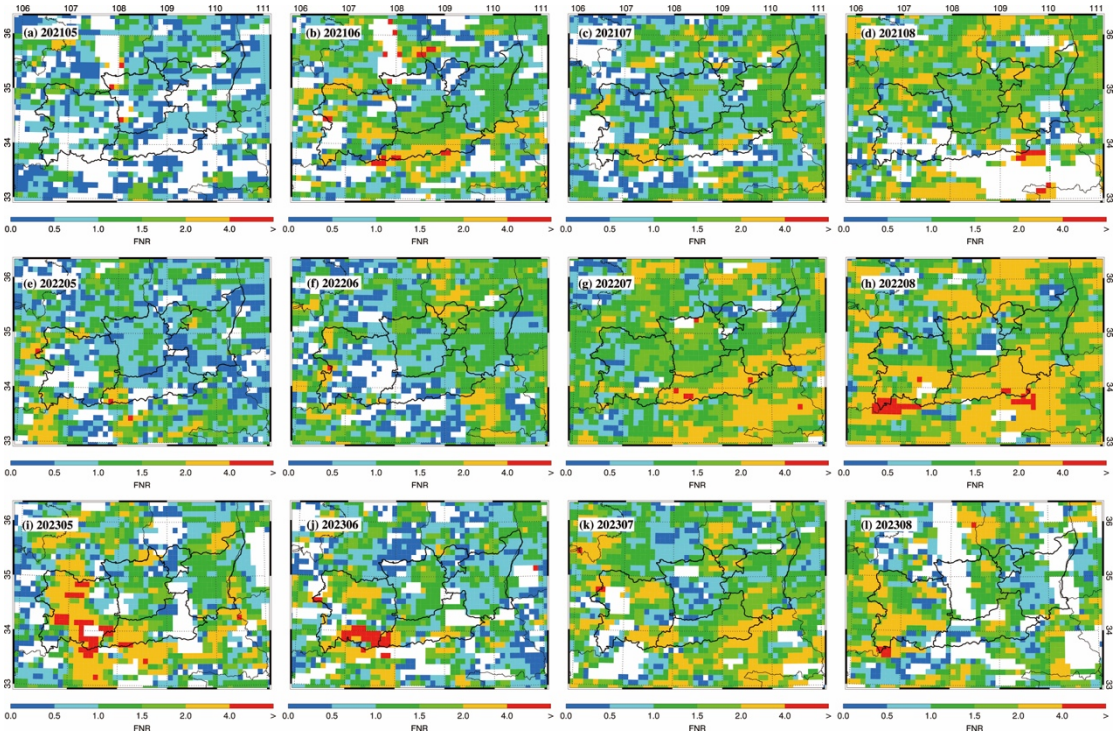

Figure S6: Spatial distribution of the satellite-derived formaldehyde-to-NO_2 ratio (FNR) over the GZB and surrounding regions. Monthly mean FNR values for the warm seasons (May–August) of (a–d) 2021, (e–h) 2022, and (i–l) 2023 are shown. FNR is calculated from tropospheric column densities of HCHO and NO_2 retrieved by the OMI sensor. According to typical threshold ranges applied in China, FNR values below 1.0 (blue tones) generally indicate VOCs-limited ozone formation regimes, values between 1.0 and 2.0 (green-yellow tones) indicate transitional regimes, and values above 2.0 (orange-red tones) indicate NO_X-limited regimes. Data gaps (white areas) are primarily due to cloud cover affecting the satellite retrievals.

Table S3 : The monthly FNR derived from satellite retrievals averaged in the GZB during warm-seasons from 2021 to 2023.

FNR	May	June	July	August
2021	0.90	1.19	1.20	1.61
2022	0.91	1.31	1.50	1.77
2023	0.97	1.20	1.43	1.51

Reference:

Hata, H., Inoue, K., Yoshikado, H., Genchi, Y., and Tsunemi, K.: Impact of introducing electric vehicles on ground-level O_3 and $PM_{2.5}$ in the Greater Tokyo Area: yearly trends and the importance of changes in the Urban Heat Island effect, Atmos. Chem. Phys., 25, 1037–1056, https://doi.org/10.5194/acp-25-1037-2025, 2025

Jin, X., and Holloway, T.: Spatial and temporal variability of ozone sensitivity over China observed from the Ozone Monitoring Instrument, J. Geophys. Res.-Atmos., 120, 7229–7246, https://doi.org/10.1002/2015JD023250, 2015.

Jin, X., Pusede, E. A., Wiedinmyer, C. J., Fischer, M. L., and Oetjen, H. J.: Evaluating a space-based indicator of surface ozone–NO_x–VOC sensitivity over midlatitude source regions and application to decadal trends, J. Geophys. Res.-Atmos., 122, 10451–10471, https://doi.org/10.1002/2017JD026720, 2017.

Rahman, M. M., Shults, R., and Ali, M. F.: Formaldehyde-to-nitrogen dioxide ratio (FNR) analysis for ozone sensitivity: a case study over Bangladesh using OMI data, Air Qual. Atmos. Health, 18, 1879–1886, https://doi.org/10.1007/s11869-025-01732-5, 2025.

Souri, A. H., Johnson, M. S., Wolfe, G. M., Crawford, J. H., Fried, A., Wisthaler, A., Brune, W. H., Blake, D. R., Weinheimer, A. J., Verhoelst, T., Compernolle, S., Pinardi, G., Vigouroux, C., Langerock, B., Choi, S., Lamsal, L., Zhu, L., Sun, S., Cohen, R. C., Min, K.-E., Cho, C., Philip, S., Liu, X., and Chance, K.: Characterization of errors in satellite-based HCHO/NO_2 tropospheric column ratios with respect to chemistry, column-to-PBL translation, spatial representation, and retrieval uncertainties, Atmos. Meas. Tech., 16, 1961–1986, https://doi.org/10.5194/amt-16-1961-2023, 2023.

2. The manuscript discusses the interactions between $PM_{2.5}$ and O_3, including aerosol radiative effects and heterogeneous uptake of HO_2 on O_3 production, but these interactions are not considered in the interpretation of ozone and secondary aerosol formation regimes. It would be helpful to discuss to what extent the substantial reduction in $PM_{2.5}$ mass from 2014–2024 may have contributed to changes in O_3 pollution, whether aerosol chemical and radiative effects affect the diagnosed sub-seasonal O_3 regimes, and how this might inform coordinated co-control strategies.

Response: We thank the reviewer for raising this important point regarding the potential role of aerosol–radiation–chemistry interactions in shaping O_3 trends and regimes, and their implications for coordinated control. We have added a new subsection (3.5.1 Impacts of Aerosol-Radiation-Chemistry Interactions) to thoroughly address these mechanisms.

L338-367: "*3.5.1 Impacts of Aerosol-Radiation-Chemistry Interactions*

The substantial decline in $PM_{2.5}$ mass in the GZB over the past decade raises the question of whether aerosol–radiation and aerosol–chemistry interactions have notably influenced the observed increase in warm-season O_3 and possibly modulated its formation sensitivity. To quantify these effects, we conduct sensitivity experiments to separately isolate (i) aerosol-induced radiative changes (A_Rad) and (ii) changes in heterogeneous HO_2· uptake on wet aerosol surfaces (A_HO_2) associated with aerosol loading variations during the warm season from 2014 to 2022. In the A_Rad experiment, all model configurations are identical to the base simulation, except that aerosol concentrations within the PBL are fixed at their 2014 levels in the aerosol–radiation transfer module. Similarly, in the A_HO_2 experiment, aerosol concentrations are fixed at 2014 levels only in the calculation of heterogeneous HO_2· uptake on wet aerosol surfaces, while all other processes remained unchanged. The resulting differences from the base case therefore represent the impacts of aerosol changes between 2014 and 2022 on MDA8 O_3 through radiative and HO_2· heterogeneous loss pathways, respectively.

Over the period 2014–2022, during which observed $PM_{2.5}$ concentrations in the

GZB have declined by approximately 21.4 μg m^{-3}, the A_Rad and A_HO_2 effects exerted comparable influences on MDA8 O_3, each contributing between 3 and 7 μg m^{-3} across most of the region. The combined influence of these two pathways results in an increase of approximately 4.0 μg m^{-3} in the mean warm-season MDA8 O_3 concentration over the GZB, with peak enhancements exceeding 7 μg m^{-3} in urban core areas with high aerosol levels during June and July (Fig. 9). Although non-negligible, this aerosol-mediated increase accounts for only 10.4 % of the total observed MDA8 O_3 rise (38.14 μg m^{-3}) during the warm seasons from 2014-2022 over the GZB. Thus, while the $PM_{2.5}$ cleanup has exerted a discernible upward pressure on O_3 via enhanced photochemistry and modified radical cycling, it is not the dominant driver of the worsening O_3 pollution; the primary factors remain the increased frequency of unfavorable synoptic conditions and changes in anthropogenic precursor emissions (Bei et al., 2022; Zhao et al., 2026).

A key follow-up question is whether these aerosol effects alter the identification of sub-seasonal OFRs. Additional sensitivity simulations for 2022, in which A_Rad and A_HO_2 are deliberately switched off, show that the combined A_Rad+A_HO_2 effect modestly suppresses MDA8 O_3 concentrations by 0.1-1.0 μg m^{-3} under current emission levels but does not change the fundamental spatiotemporal progression of the O_3 formation sensitivity (Fig. S7). This indicates that the chemical sensitivity of O_3 production to its precursors is primarily governed by the evolving balance between NO_X and VOCs under the prevailing meteorology, rather than by aerosol-mediated perturbations under contemporary pollution levels.

Therefore, although the historical $PM_{2.5}$ reduction has provided a modest boost to O_3 concentrations, it has not reshaped the intrinsic, meteorologically-driven transitions in OFR. This finding supports the use of OFR diagnostics, which are largely insensitive to aerosol loading in the current environment, as a reliable basis for designing seasonally adaptive control strategies. ”

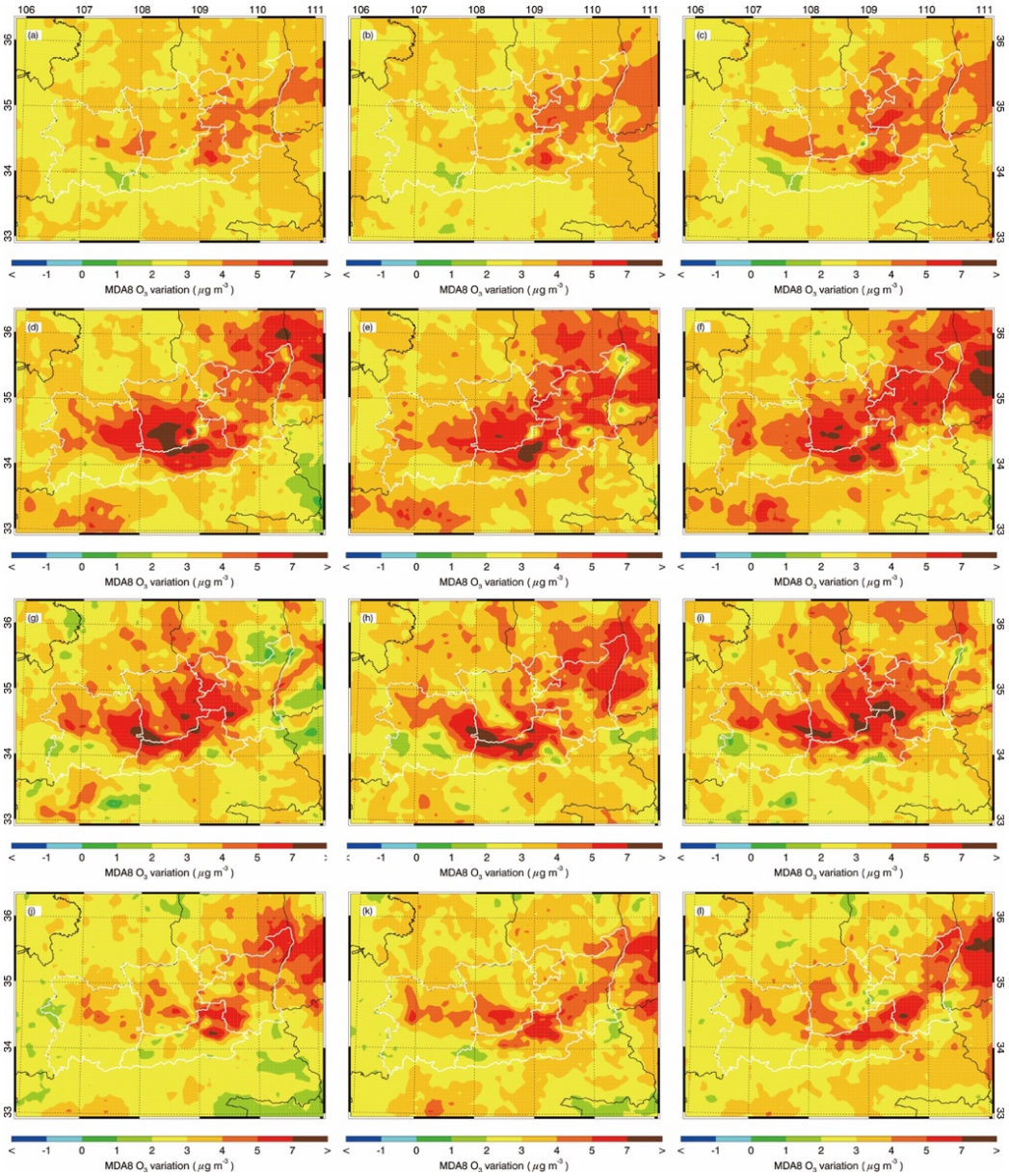

Figure 9: Impacts of aerosol changes on warm-season (May–August) MDA8 O_3 concentrations over the GZB during 2014–2022. Panels (a), (d), (g), and (j) show the changes in MDA8 O_3 attributable to aerosol-radiation effects associated with aerosol variations for May, June, July, and August, respectively. Panels (b), (e), (h), and (k) show the corresponding MDA8 O_3 changes driven by variations in heterogeneous uptake of HO_2 radicals on wet aerosol surfaces induced by aerosol changes. Panels (c), (f), (i), and (l) present the combined effects of aerosol-radiation interactions and HO_2 heterogeneous uptake changes on MDA8 O_3 concentrations for the corresponding months.

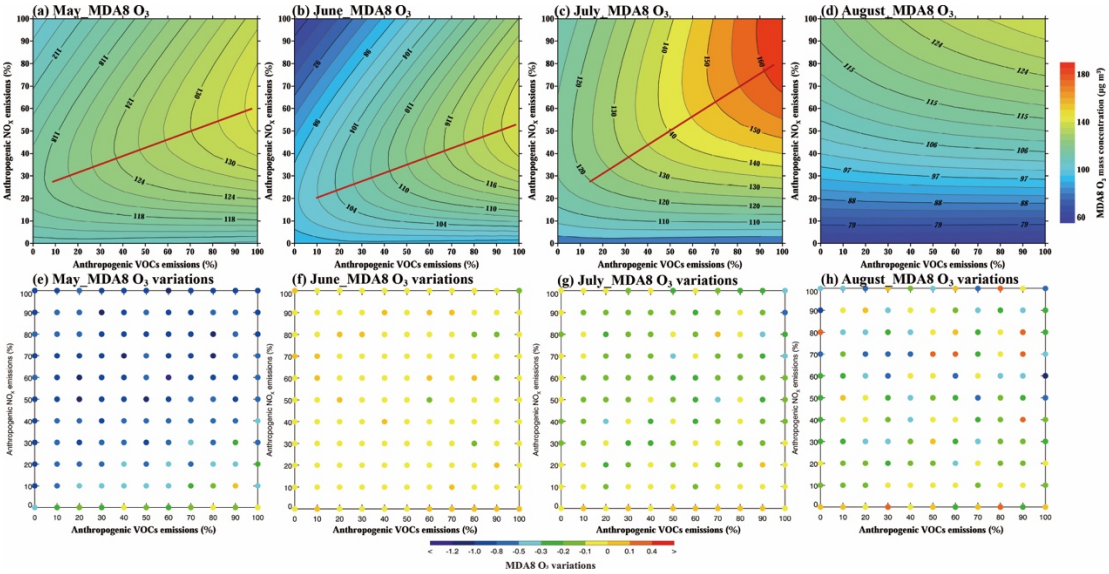

Figure S7: MDA8 O_3 isopleth profiles (μg m^{-3}) and corresponding MDA8 O_3 concentration variations in urban areas of the GZB during high-O_3 pollution episodes in 2022, with aerosol-radiation effects and heterogeneous uptake of HO_2 radicals on wet aerosol surfaces associated with aerosol variations excluded. Panels (a) and (e) show results for May, (b) and (f) for June, (c) and (g) for July, and (d) and (h) for August.

Reference:

Zhao, C., Sun, Y., Yang, J., Li, J., Zhou, Y., Yang, Y., Fan, H., and Zhao, X.: Decadal evolution of aerosol-mediated ozone responses in Eastern China under clean-air actions and carbon-neutrality policies, Atmos. Chem. Phys., 26, 1301–1318, https://doi.org/10.5194/acp-26-1301-2026, 2026.

Bei, N., Liang, J., Li, X., and Wang, R.: Worsening summertime ozone pollution in the Guanzhong Basin, China from 2014 to 2018: impacts of synoptic conditions and anthropogenic emissions, Atmos. Environ., 274, 118974, doi:10.1016/j.atmosenv.2022.118974, 2022.

3. Other minor comments:

19: dominate should be dominant

Response: corrected.

216–222: These sentences are repeated.

Response: We have removed the repeated statements.

277–289: This paragraph reads more like background rather than results.

Response: We have removed the paragraph in the results.

300: Table 4 should be Table 3.

Response: corrected.

Section 3.5: The discussion of secondary aerosol formation regimes is largely descriptive. Additional explanation of the chemical or meteorological processes driving variability in SA regimes would improve the interpretation.

Response: We have added related discussion in Section 3.5 as follow,

L379-388: "*The observed spatiotemporal evolution of SAFR can be interpreted in the context of the seasonal progression of key chemical and meteorological drivers. The NO_X-limited regime in early summer is likely associated with an enhanced contribution of nitrate to secondary aerosols, under conditions where SA formation remains sensitive to NO_X through HNO_3 production and subsequent gas–particle partitioning favored by relatively lower temperatures, higher humidity, and weaker photochemical activity. As solar radiation and temperature increase in June, the enhanced atmospheric oxidation capacity, together with temperature-dependent VOCs and biogenic emissions, promotes SOA formation, leading to a shift toward a VOCs-limited SAFR. The persistent VOCs sensitivity in WN into July reflects its relatively high NO_X emissions, which decrease the local VOCs/NO_X ratio and thereby reinforce VOCs-limited chemistry. By late summer (August), warmer and more humid conditions increase aerosol liquid water content and favor efficient nitrate formation and partitioning, contributing to a renewed tendency toward NO_X-sensitive SAFR.*"

Figure S4: The x-axis time label is incorrectly marked as 2018.

Response: We have revised the figures as follows,

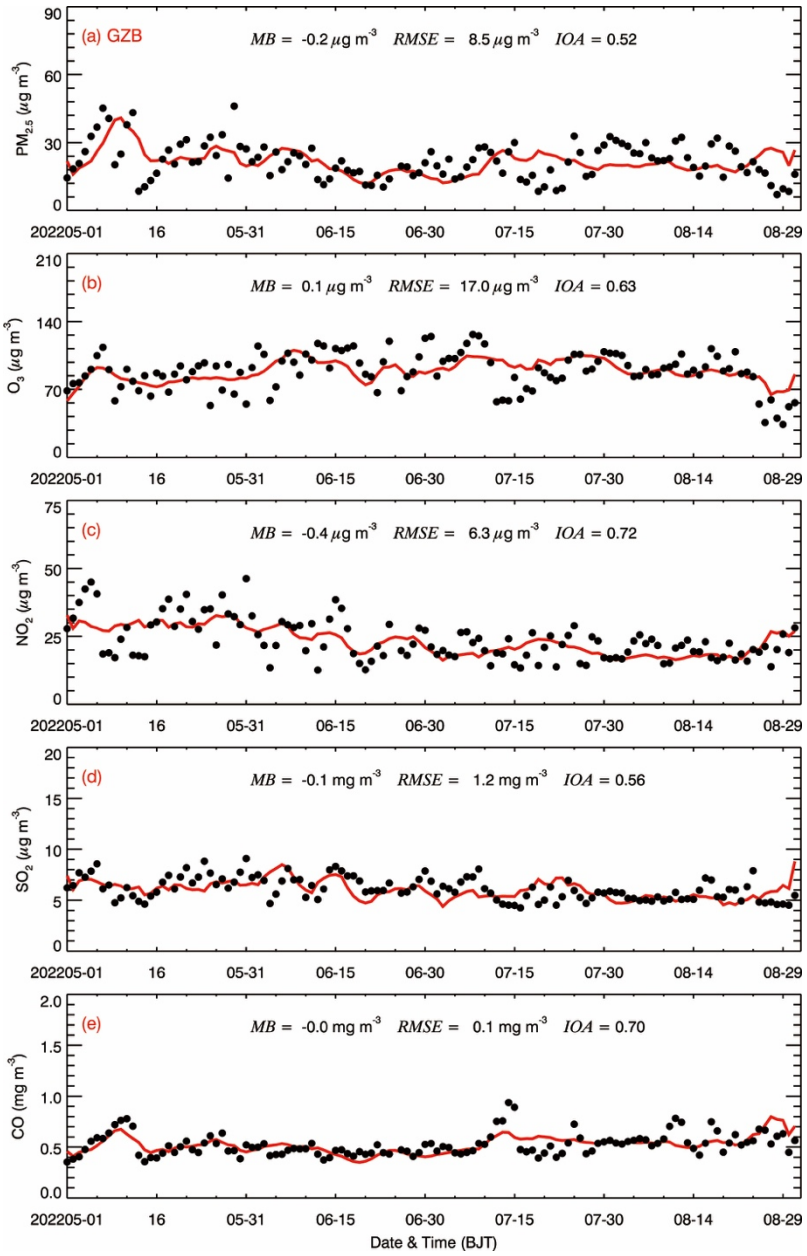

Figure S4: Diurnal profiles of measured (black dots) and predicted (red line) (a) $PM_{2.5}$, (b) O_3, (c) NO_2, (d) SO_2, and (e) CO concentrations averaged over all ambient monitoring stations in the GZB from May to August 2022.

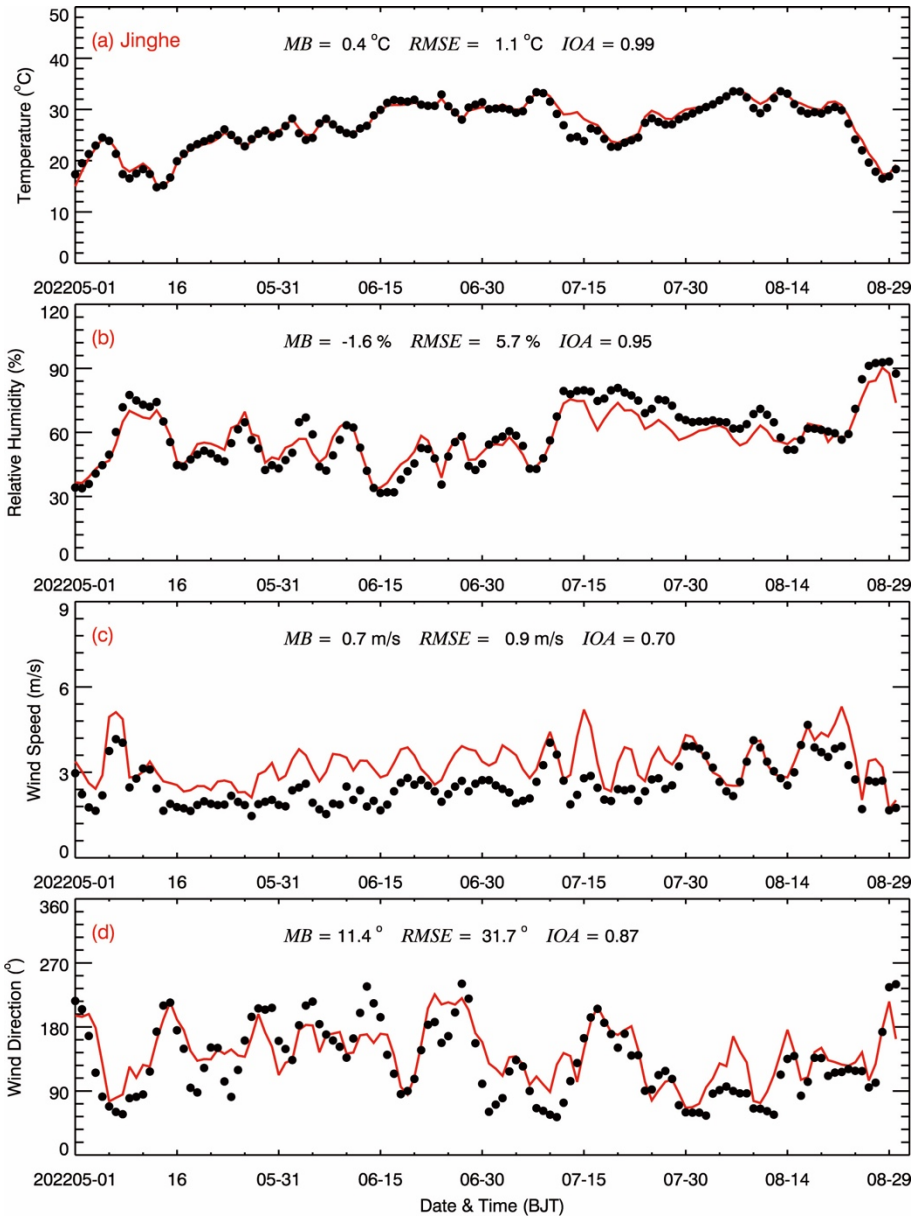

Figure S2: Temporal variations of predicted (red) and observed (black) (a) temperature at 2 m, (b) relative humid at 2 m, (c) wind speed and (d) wind direction at 10 m at Jinghe meteorological monitoring site from May to August 2022. The model performance statistic metrics of MB, RMSE and IOA are also shown.